CHEMISTRY
A EUROPEAN JOURNAL

DOI: 10.1002/chem.200801133

Regio-, Peri-, and Torquoselectivity in Hydroxy Heptatrienyl Cation Electrocyclizations: The Iso/Homo-Nazarov Reaction

Olalla Nieto Faza, Carlos Silva López, Rosana Álvarez, and Ángel R. de Lera*[a]

Abstract: The electrocyclizations of 1- and 3-hydroxyheptatrienyl cations have been computationally studied at the B3LYP/6-311G(d) level. The 1-hydroxy system clearly favors a $4\pi e^-$ over a $6\pi e^-$ process, while for the 3-hydroxy isomer these mechanisms compete. Substituents can either enhance or invert this periselectivity through steric or electronic effects, respectively. Houk's model of torquoselectivity helps to explain the activation energy differences between the alternative $4\pi e^-$ electrocyclizations available for each system. The cyclopentenyl cations thus obtained can evolve, either through intramolecular trapping by the vinyl group or by 1,3-proton migration, along reaction coordinates which could correspond to either very asynchronous concerted mechanisms, or two-step reactions with very shallow or non-existent intermediates.

Keywords: cycloaddition · electrocyclic reactions · pericyclic reactions

Introduction

The Nazarov reaction has recently enjoyed considerable attention,[1–3] and so have the possible formations of the cyclopentenyl cation obtained from the $4\pi e^-$ electrocyclization. A considerable amount of work has been directed towards the study of different ways of capturing this cationic intermediate, resulting in a wealth of examples of "interrupted Nazarov" processes,[1,2,4–8] that have significantly expanded the synthetic scope of this reaction. Most examples are intermolecular captures of the allyl cation with nucleophiles such as water,[9] amines,[7] azides,[6] halides[8] or other groups like allylsilanes,[10] or alternate processes like cycloaddition reactions,[11] but there are also reports of intramolecular trapping reactions, via Wagner–Meerwein rearrangements[12,13] or attacks of vicinal nucleophilic groups (olefins, arenes).[4,14]

In the framework of our group's experience in the synthesis and reactivity of polyenes and following our work on the electrocyclization of hydroxypentadienyl cations[15] we set out to extend this last study to the ring-forming reaction of isomeric hydroxyheptatrienyl cations. These vinylogous Nazarov (3-hydroxy) and iso-Nazarov (1-hydroxy) systems enrich the mechanistic possibilities and provide the structural elements for a complex set of electrocyclizations. In these systems, the presence of a further unsaturation along the chain, ending on a vinyl substituent upon the cyclopentenyl ring formation, makes the potential intramolecular capture of the intermediates by the olefin a process on the line of the novel class of "interrupted Nazarov" reactions (Scheme 1) recently reported by West et al.[14] where a non-conjugated alkene held near the dienone nucleus undergoes intramolecular trapping of the Nazarov 2-oxido cyclopentenyl intermediate. The structural consequences of these cascade reactions are complex bicyclic or tricyclic products with a controlled stereochemistry.

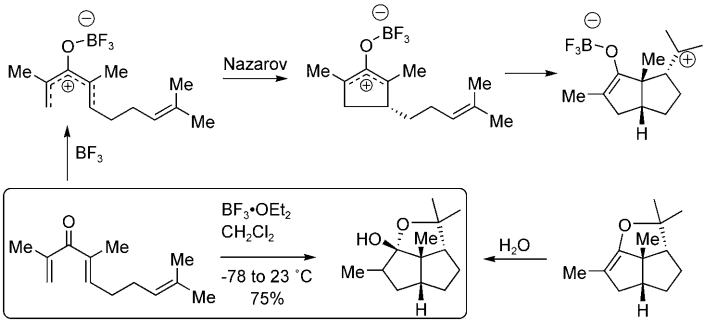

Scheme 1. The "interrupted" Nazarov reaction.[16] One of the first examples of deliberate trapping of the Nazarov oxyallyl intermediate.

[a] Dr. O. N. Faza, Dr. C. S. López, Dr. R. Álvarez, Prof. Dr. Á. R. de Lera
Departamento de Quìmica Orgánica
Facultad de Química, Universidade de Vigo, Lagoas Marcosende, 36310, Vigo, Galicia (Spain)
Fax: (+34) 986-811940
E-mail: qolera@uvigo.es

Also of interest in these longer polyenes is the periselectivity of the cyclizations. While it is generally accepted that when several geometrically accessible and symmetry-allowed transition structures are available for a given system, it will evolve through the path with a more extended conjugation, these assumptions are usually founded in data collected about neutral species.

Examples of periselectivity favoring the process involving the greater number of atoms have been reported for similar anionic conjugated polyenes (conjugated pyridinium ylides, isoelectronic with heptatrienyl anion) where the formation of seven-membered rings ($8\pi e^-$) competes with five-membered rings ($6\pi e^-$)[17] or for the cyclization of neutral substituted octatetraenes.[18] Nevertheless there are systems, such as conjugated azomethine ylides, where the difference in activation barriers for the alternate processes (1,7- and 1,5-electrocyclizations) is reduced and the product distribution depends heavily on the substituents.[19]

An explanation for the periselectivity is usually based on the stabilization of the longer conjugated system in the transition structure (the alternative paths would imply breaking the conjugation present in the reactant) or the maximum overlap of the frontier molecular orbitals, whose coefficients are the highest at the terminal carbons on a polyene system,[20] the geometrical preference for helical- versus boat-like conformations for the transition structures (conrotatory vs. disrotatory), or the substituent effects on the balance between orbital- or charge-controlled cyclizations which would yield different products.[19] We would like to examine the periselectivity of these cationic cyclizations, in which we anticipate that the stereoelectronic effects favoring a helical transition structure for the transition state (found in the conrotatory $4\pi e^-$ cyclization) oppose the preference for extended conjugation (in the $6\pi e^-$ cyclization).

Although no comprehensive study of these systems has been published, there are examples of synthetic applications for some of the reactions described in this paper. Of great relevance is the work by Trauner et al. on the synthesis of crispatene natural products (Scheme 2).[21,22] The key step in this approach can be defined as a $4\pi e^-$ pentadienyl cation electrocyclization followed by the capture of the resultant cyclopentenyl cation by a neighboring enolate ester, which leads to a complex bicyclo[3.1.0]hexene derivative of controlled configuration.

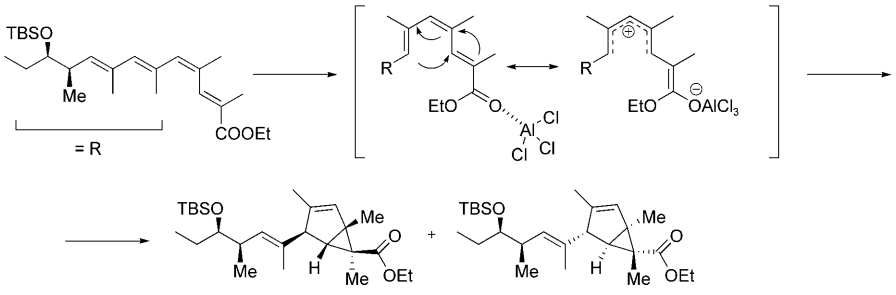

Scheme 2. Cyclization step in the synthesis of the crispatene core by Trauner et al.[21,22]

In this work, we will focus on three aspects of the electrocyclization of hydroxyheptatrienyl cations (Scheme 3):

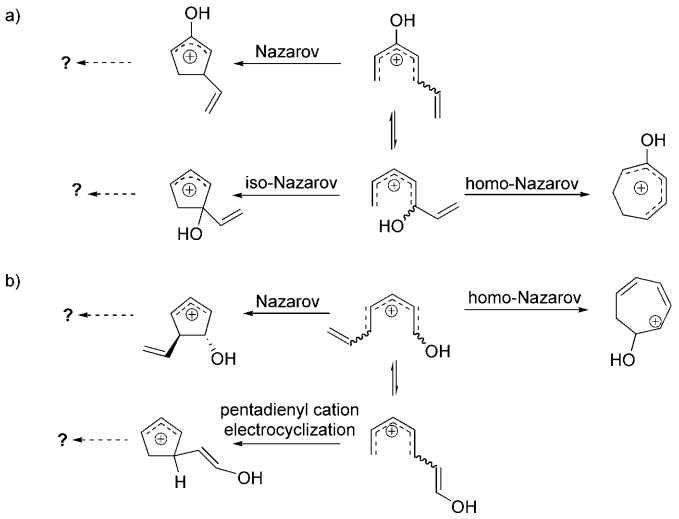

Scheme 3. Periselectivity in the 3-hydroxy- (a) and the 1-hydroxyheptatrienyl cation (b) cyclizations and unanticipated evolution of the cyclopentenyl intermediates with potential involvement of the vinyl groups.

- A comparison of the $4\pi e^-$ cyclizations with those reported for their lower homologues hydroxypentadienyl cations, with special emphasis on the torquoselectivity.
- The competition between $4\pi e^-$ and $6\pi e^-$ electrocyclizations (periselectivity).
- The evolution of the pentadienyl cation products of the $4\pi e^-$ cyclizations, through cationic cascades resulting in polycylic structures.

Results and Discussion

The complexity of the study is illustrated by the evolution of the 1- and 3-hydroxyheptatrienyl cations selected as starting materials. Two electrocyclic manifolds enter into competition for each delocalized cation: the 7-atom-6-electron and the 5-atom-4-electron processes.[1,2] We discarded the occurrence of the 3-atom-2-electron path, since the cyclopropyl cation has been shown to spontaneously open due to the release of ring strain.

As the main purpose of this work is the study of the competing electrocyclizations and the factors affecting their relative energies or selectivities, we will separate the study of the reactions of the 1-hydroxyheptatrienyl cation from those of the 3-hydroxyheptatrienyl cation. In addition, for each of

these structures the reactions where the hydroxyl is located on one of the cyclizing termini were separated from those where it is elsewhere. In so doing, the complex configurational/conformational equilibria involved are somehow ignored. The first consideration involves the interconversions of the different *cis–trans* isomers of these highly delocalized polyenyl cations. The energy of these isomerizations are relatively low compared with those common for non-conjugated alkenes, resulting in the possibility of conformational scrambling of the initial heptatrienyl cation. Only some of the possible transition structures for these interconversion processes have been calculated and, where appropriate, they appear in the Tables. If the linear system were used, activation barriers such as 7.83 kcal mol^{-1} for the rotation of the C_2–C_3 bond (**1F** to **1G**) or 11.15 kcal mol^{-1} for the rotation of the C_5–C_6 bond (**1B** to **1D**), much lower than the cyclization activation barriers, would guarantee that only the cyclization product of the most stable reactive conformer is obtained. Nevertheless, since it is tethered (or conformationally locked) versions of these systems that would be ideally suited for synthetic applications, the less favorable cyclizations are still described.

Cycloisomerizations of the 3-hydroxyheptatrienyl cation: This system results in mechanisms similar to the more conventional Nazarov and iso-Nazarov pentannelations described in our previous paper.[15] The different processes this structure can undergo are displayed in Scheme 4, where the following notation has been adopted: isomers **1A** through **1D** and **1E** through **1H** are used to indicate the vinyl-Nazarov and vinyl-iso-Nazarov manifolds, respectively, which differ in the position of the hydroxyl with respect to the cyclizing atoms. Along the mechanistic pathway, cascade cationic cyclizations are sometimes observed and the intermediate products found along these sequences are indicated with consecutive numbers (**2** to **4**). The competition between the 4e$^-$ and the 6e$^-$ cyclizations (**1G–2E** vs. **1G–2C**) will be discussed in the next section, as the involved conformer is present in the two mechanisms.

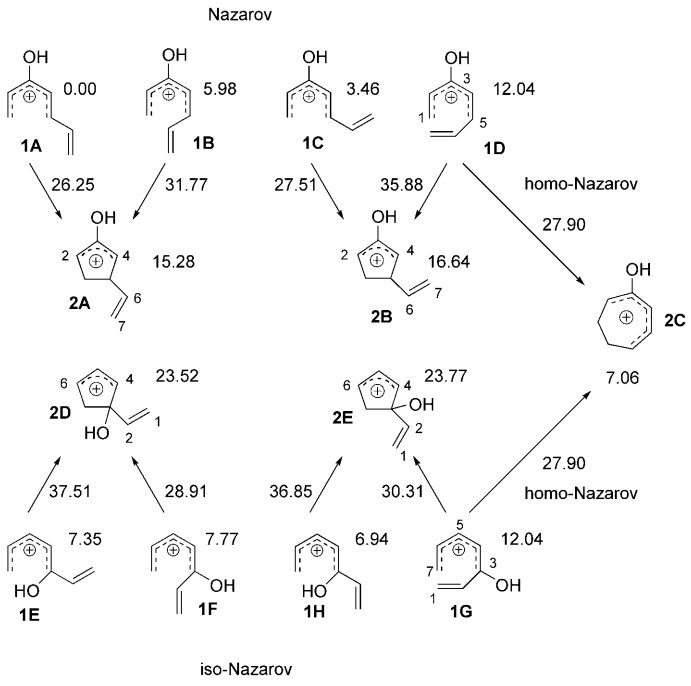

Scheme 4. Cyclizations of the 3-hydroxyheptatrienyl cation. The free energies of the depicted stationary points are shown on the scheme in kcal mol^{-1}.

First step: Nazarov versus iso-Nazarov cyclization: In the set of isomers (**1A–1D**), which most closely resembles a Nazarov reaction, the cyclization takes place between C_1 and C_5. If the extended chain is chosen as the reference from which free energies are calculated (thus setting a common energy origin, the most stable conformer **1A**, for the iso-Nazarov and Nazarov manifolds), the electrocyclic processes in which the vinyl group is located outwards are favored with respect to those where it points inwards. As stated elsewhere,[15] this phenomenon can be easily explained resorting to both steric (less congestion in the transition structure and s-*trans* conformations of the alkenes more favorable than the alternate s-*cis*) and electronic arguments (the slightly electron-donor vinyl preferring outwards rotation). However, if we consider the isomers in Scheme 4 as the starting point for each cyclization, the lowest reaction barrier is found for the most unstable, **1D**.

For the set of conformers of the 3-hydroxyheptatrienyl cation (**1E–1H**), which would evolve through the alternative iso-Nazarov cyclization, both a vinyl and a hydroxyl group are located at one terminus of the cyclizing cationic pentadienyl system. The conformers where the hydroxyl group is located inwards display much higher barriers ($\Delta\Delta G^{\neq}$ between 8.76 and 11.89 kcal mol^{-1}) than their outwards counterparts, another example of torquoselectivity due to the classical closed-shell repulsion first described by Houk for the ring opening of substituted cyclobutenes.[23] This stereoelectronic effect is more marked when the substituent is a better donor, hence the preference for an inwards vinyl, even if it is an electron-donor substituent itself. As for the s-*cis*/s-*trans* conformation of the vinyl group, the preferred orientation is *syn* to the less bulky hydroxyl in the minima (energies of 6.94 (**1H**) vs. 7.35 (**1E**) kcal mol^{-1} and 7.77 (**1F**) vs. 12.04 (**1G**) kcal mol^{-1}). This steric effect is in **1G** enhanced by the tendency to planarity imposed by conjugation in the minima, yielding a rather strained helical structure. In the corresponding transition state, these planarity requirements are relaxed, since the conjugation with the terminal vinyl group is lost as the reaction proceeds, resulting in the lowest barrier for the four 4e$^-$ processes in this group. However, if one considers the open chain as the reference for calculating activation barriers (the correct choice for the linear systems), **1F–2D** would be the favored cyclization among the vinyl-iso-Nazarov processes.

Another relevant aspect of these cyclizations is their remarkable periselectivity. When comparing the reaction barriers obtained with the same reference (e.g., ΔG values in

Table 1), we observe that the activation energies are in general smaller for the Nazarov cyclizations. However, this tendency is reversed when dealing with transition structure energies relative to the nearest minimum. In this last case, the barriers are lower for the iso-Nazarov processes, as would be expected from the higher polarization of the system and the instability of the reacting conformations involved. This last result is fully consistent with the difference (about 5 kcal mol^{-1}) in the barriers calculated for the analogous hydroxypentadienyl electrocyclizations.[15]

Table 1. Thermodynamic data for the reactions in Scheme 4. The units are kcal mol^{-1} and the reference for relative energies is **1A**.

Structure	ΔG	$\Delta G^{\neq}$	Structure	ΔG	$\Delta G^{\neq}$
1A	0.00		**1H**	6.94	
1B	5.98		**1F**	7.77	
1C	3.46		**1E**	7.35	
1D	12.04		**1G**	12.04	
1A–2A	26.25	26.25	**1H–2E**	36.85	29.91
1B–2A	31.77	25.79	**1F–2D**	28.91	21.15
1C–2B	27.51	24.05	**1E–2D**	37.51	30.16
1D–2B	35.88	23.84	**1G–2E**	30.31	18.27
1D–2C	27.90	15.86	**2D**	23.52	
1D–2C′	37.07	25.03	**2E**	23.77	
2A	15.28		**1F–1G**	15.60	7.83
2B	16.64				
2C	7.06				
1B–1D	17.13	11.15			

Analysis of geometric parameters (see Supporting Information), reveals a pattern of π-bond "localization" in the minima (all isomers of **1**) consistent with "localized π-bonds between C_1–C_2, C_4–C_5 and C_6–C_7, with the cation at C_3 stabilized by the heteroatom. However, in the transition structures, the behaviour differs for the two groups **1A–1D** and **1E–1H**. The former can be best depicted as a completely delocalized pentadienyl cation (the bond equalization is much more important in these structures than in their iso-Nazarov counterparts) substituted with a non-conjugated vinyl group, while in the latter, the pattern of the minima is conserved in the transition structures, which could be alternatively characterized as the attack of the C_6–C_7 alkene to the allyl cation C_3-C_4-C_5, leaving thus the new cation in the product on C_6. Analysis of NBO charges supports these arguments. The resulting difference between the transition structures corresponding to the cyclizations of the **1A–1D** and the **1E–1H** isomers can be correlated with both, the greater distances between the bonding atoms that indicate an earlier transition structure and a less advanced electronic rearrangement in the latter, and the fact that the electronic distribution in the **1E–1H** isomers and the corresponding transition structures is conserved in the cyclopentenyl products (with the exception of the π–σ transformation, inherent to the electrocyclic process).

Worth of notice is the dihedral angle $\measuredangle_{1234}$ in iso-Nazarov and $\measuredangle_{4567}$ in Nazarov, which can be taken as a measure of the conjugation of the pendant "vinyl substituent" to the main pentadienyl chain. This angle, nearly planar in the minima (with the exception of **1G**, where this would imply a very strained structure) increases considerably in the transition structure. At this stage conjugation can be considered almost completely interrupted and the system behaves as a substituted pentadienyl cation instead of a conjugated heptatrienyl cation where the six π electrons contribute to the pericyclic transition state.

Since in iso-Nazarov reactions we are dealing with doubly-substituted cyclizing systems where stereoelectronic effects are complex, there is not a direct correlation between the forming bond lengths in the transition structure, taken as reaction advance indices, and the activation energies.

First step: 4πe⁻ versus 6πe⁻ reactions, Periselectivity of cationic versus neutral electrocyclizations: Extrapolation of the results obtained for neutral systems,[18] led us to expect 6πe⁻ cyclizations as the preferred processes. The calculated reaction barriers confirm this hypothesis if the most unstable isomer **1D** is chosen as the reactant, since the 18.27 or 23.84 kcal mol^{-1} barriers corresponding to the 4πe⁻ cyclization transition structures **1G–2E** and **1D–2B**, respectively, cannot compete with the 15.86 kcal mol^{-1} required for the formation of **2C**. However, if we consider the possibility of configurational interconversions, this preference is overcome by the strict conformational requirements for an all-s-*cis* conformation of the polyenyl cation, resulting in a complex mix or products, being the most abundant the result of a vinyl-Nazarov cyclization (84% **1A–2A**, 10% **1C–2B**, 5% **1D–2C** and 1% **1F–2D** if we consider a Maxwell–Boltzmann distribution at 25°C).

Nevertheless, it should not come as a surprise if by careful modifications of the heptatrienyl cation substrate that destabilize its all-*s*-*cis* conformation and, consequently, the transition structure leading to **1D–2C**, improved selectivity in the cyclopentenyl product was achieved. Other structural variation might alternatively favor the transition structure for the cycloheptadienyl system **1D–2C**, and revert the periselectivity.

To test this hypothesis, we located the transition structures for the 6πe⁻ and the most favorable 4πe⁻ electrocyclizations for some substituted 3-hydroxyheptatrienyl cations (the substitutions are displayed in Figure 1 and the energy values are collected in Table 2).

As can be seen from the values in Table 2, substitution enhances in most cases the $\Delta G^{\neq}$ differences (1.65 kcal mol^{-1} for the model system) without altering the previous order, since the pentannelation is the preferred process in all systems with the exception of **e**.

The presence of bulky substituents on the cyclization termini clearly favors 4e⁻ cyclization with respect to the 6e⁻ process, as can be inferred from the $\Delta\Delta G^{\neq}_{6-4}$ values obtained for **a** and **f**. This steric effect albeit less dramatic, is still important in the **b** and **c** series, where the steric demands of the *t*Bu group force a closing of the C_3-C_4-C_5 angle (α_{345} = 119.9° for **1D–2C** (**b**) and α_{456} = 121.7°, compared with the

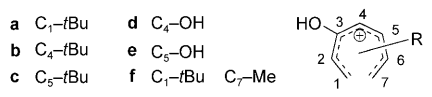

Figure 1. Substituted 3-hydroxyheptatrienyl cations (**a**–**f**) for the study of the periselectivity.

Table 2. Relative thermodynamic data for the transition structures for the electrocyclic ring closure of the substituted 3-hydroxyheptatrienyl cations shown in Figure 1. As the target is assessing the effect of substituents on the preference between four and six-electron processes, only competing transition states (with the structures depicted in Scheme 4) were computed, and the energies noted (in kcal mol^{-1}) are referred to the lowest energy transition structure.

	Structure	ΔG		Structure	ΔG
	1D–2C	3.67		**1D–2C**	5.38
a	**1A–2A**	0.00	**b**	**1A–2A**	1.16
	1G–2E	1.37		**1G–2E**	0.00
	1D–2C	2.98		**1D–2C**	2.54
c	**1A–2A**	15.42	**d**	**1A–2A**	0.00
	1B–2A	12.99		**1G–2E**	2.94
	1G–2E	0.00			
	1D–2C	0.00		**1D–2C**	9.54
e	**1B–2A**	3.10	**f**	**1A–2A**	0.00
	1G–2E	3.57		**1G–2E**	3.59

128.7 and 129.5° values for the equivalent angles in the non-substituted transition structure), thus destabilizing the seven-membered ring structure needed for the 6e$^-$ cyclization. Important is the slight increase in $\Delta\Delta G^{\ddagger}_{6-4}$, which results from donor groups on C_4, noticeable in **d** and **b**, reinforcing in the latter the steric effect of the *t*Bu substituent.

The most remarkable effect, however, is that observed in **e**, where the general preference for five-membered ring formation is reversed, favoring the 6e$^-$ cyclization. The resultant $\Delta\Delta G^{\ddagger}_{6-4}$ value of -3.10 kcal mol^{-1} can be readily explained by using torquoelectronics arguments. When a donor substituent is located on C_5, a donor group is forced to rotate inwards upon any conceivable 4e$^-$ electrocyclization: either the hydroxyl group on C_3, the new substituent on C_5, or one of the vinyl groups on any of these two positions will incur in the usual two-orbital-four-electron destabilizing interaction in the transition structure. The 4.5 kcal mol^{-1} difference from the $\Delta\Delta G^{\ddagger}_{6-4}$ with and without the OH on C_5 agrees well with the values observed for the torquoselectivity preferences in the in and out rotations of vinyl groups upon the non-substituted cyclizations of 3-hydroxy heptatrienyl cations discussed above.

Besides the disrotatory transition structure (**1D–2C**) for the hydroxy cycloheptadienyl formation, another saddle point (**1D–2C′**), which is 9.17 kcal mol^{-1} higher in energy than the former (Table 1), was found that would correspond to the Woodward–Hoffmann forbidden conrotatory 6πe$^-$ electrocyclic reaction (see Scheme 5).

In fact, this "conrotatory" (it displays the helical geometry characteristic of conrotations) seven-atom 6e$^-$ cyclization features a transition structure with little resemblance to an ordinary electrocyclization: the termini of the polyene chain are barely rotating (it is difficult to define it either as a conrotatory or a disrotatory process), only changing their hybridization and it looks as if a C_1–C_6 bond were being formed, instead of the expected C_1–C_7. Examination of the IRC for this mechanism (Figure 2), leads to the incipient

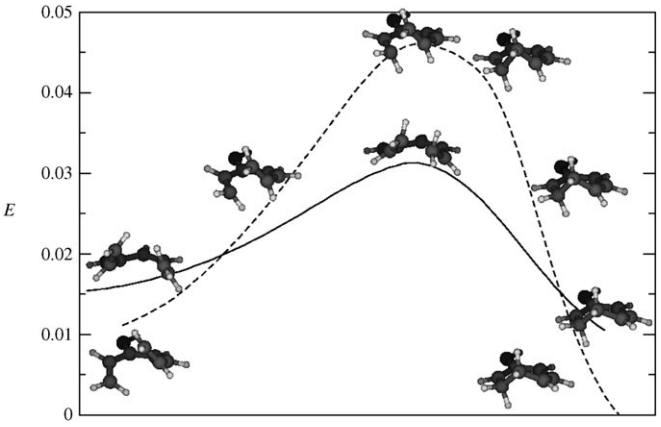

Figure 2. Representation of the structural changes along the IRC corresponding to the transition structures **1D–2C** (——, disrotatory) and **1D–2C′** (-----, conrotatory). The energy values are relative to the lower energy point in the graph and noted in Hartrees.

formation of a geometrically favored six-membered ring, which evolves before completion (there are no intermediates) to the expected seven-membered cyclic product (**2C**), which has a much more favorable charge distribution, with the cation delocalized along the hydroxy pentadienyl backbone instead of sitting on a terminal methylene with no stabilization whatsoever. In Figure 3, the evolution of the NBO atomic charges along the reaction coordinate can be compared to the progress of r_{16} and r_{17} distances, supporting this argumentation. This kind of complex reaction coordinate, will be also found for the evolution of the products of the pentannelations.

The much lower $\Delta\Delta G^{\ddagger}$ forbidden–allowed found for this cationic 6πe$^-$ system relative to the neutral 8πe$^-$ cyclization of (2*Z*,4*Z*)-octatetraene (9.17 vs. 27.4 kcal mol^{-1}),[18] can be explained by the rare occurrence of this seemingly indirect mechanism, together with the high-energy boat conformation (see Scheme 5) of the disrotatory transition structure for the octatetraene 8πe$^-$ cyclization.

A representation (see Figure 4) of the NICS values along a line normal to the molecular plane traversing the incipient ring center for the competing transition structures **1G–2E** and **1G–2C** also points towards a preferred non-pericyclic (the transition structure shows a slight antiaromaticity) mechanism for the conrotatory seven-atom cyclization (**1G–2C′**).

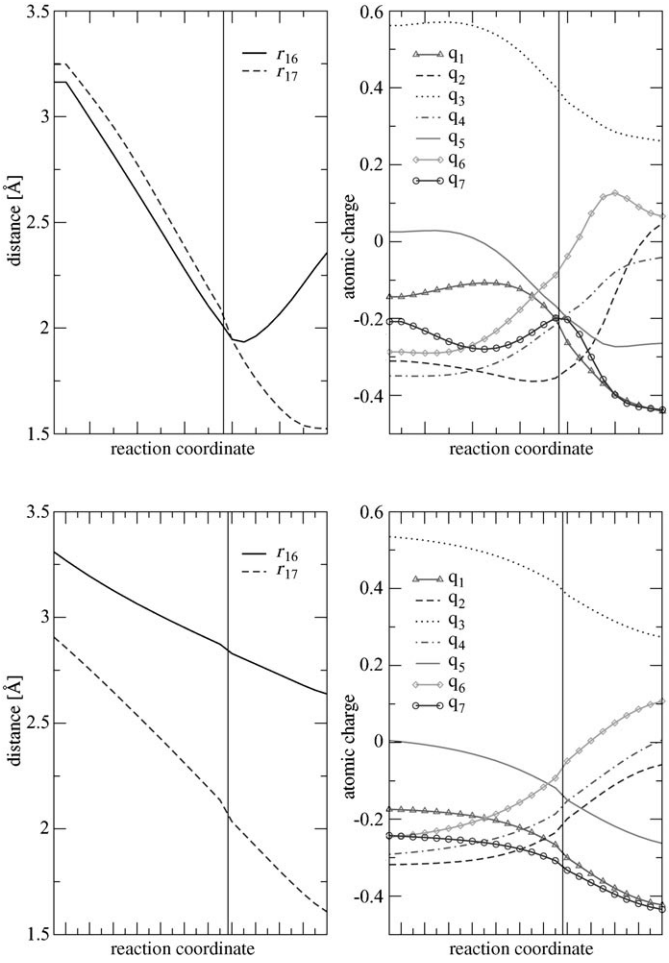

Figure 3. Evolution of the r_{16} and r_{17} distances and the NBO atomic charges on the carbon chain along the IRC corresponding to **1D–2C′** (conrotatory, top panels) and **1D–2C** (disrotatory, bottom panels). The transition state location is shown by means of a vertical line in the plots.

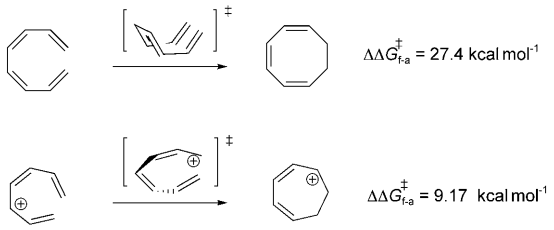

Scheme 5. "Forbidden" electrocyclizations for neutral and cationic conjugated systems, with a representation of the geometry requirements, together with the values of the preference for the allowed processes (conrotatory for the $8\pi e^-$ and disrotatory for the $6\pi e^-$ system).

Second Step: Evolution of the cyclopentenyl cation: The introduction of the terminal vinyl group, which allows the intramolecular trapping of the cyclopentenyl cations **2A** and **2D**, adds a layer of complexity to the studied systems, as a new set of cationic processes can take place before the conventional termination step (the evolution to a cyclopentenone ring, the usual product of a Nazarov reaction). We have explored the generation of diversity in these cationic cascades and estimated their activation energies and reaction paths. Although for the parent system **1**, some mechanistic choices are shown not to be competitive in the usual reaction conditions, new experimental settings or design substrates could be devised to promote them and explore these synthetically appealing possibilities. Therefore, for each of these vinyl-hydroxycyclopentenyl cations **2A** and **2D**, we set out to describe four possible scenarios for the vinyl trapping of the cation which correspond to the different combinations arising from the two extrema of the alkene trapping the endocyclic allyl cation at the two terminal carbons. The newly generated carbocation can experience further rearrangements. In some cases, the comparative ease of the carbocation migrations in these systems can lead to reaction paths formally corresponding to two-step transformations, where no intermediate could be found. Therefore, to aid in the interpretation of the skeletal transformation, the newly formed bonds are represented in gray in Schemes 6 and 7 and the atom numbering is preserved along the cascade, regardless of the compounds′ nomenclature.

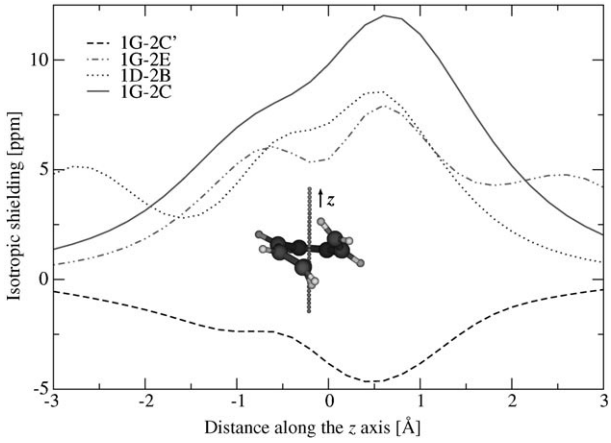

Figure 4. Representation of the NICS versus the distance along an axis normal to the molecular plane that contains the center of the ring for **1G–2C** (the transition structure corresponding to the heptannelation), deemed to be aromatic, and **1G–2C′**, which shows no aromatic features. The representation of the competing $4\pi e^-$ pentannelations (**1G–2E** and **1D–2B**) are also shown for comparison.

Although IRC calculations carried out on these transition structures verified that they connected the proposed minima and a search for minima along the reaction coordinates yielded no results, the existence of intermediates cannot be precluded. However, they would likely correspond to shallow minima in the potential energy surface, connected to the stationary points already described through very low barriers. We could be dealing then with either very asynchronous concerted reactions or two step processes with either very shallow or non existent intermediates.[24]

Despite the complex reaction paths, which not always correspond to the original mechanistic propositions, we still keep the first proposed classification in order to better com-

pare and display the changes in bonding that are taking place. Schemes 6 and 7 depict the cationic cascades arising from intramolecular trapping by the vinyl group of the (hydroxy)cyclopentenyl cations that originate in the Nazarov (iso-Nazarov) electrocyclic reaction of (*Z*)-3-hydroxyheptatrienyl cations **1**.

The most favored processes for the evolution of **2A** and **2D** are those characterized by the transition structures **2A–3B** and **2D–3E** with activation barriers of 20.93 and 18.54 kcal mol^{-1}, respectively. Increasing activation energies are computed for other alternatives in the manifold: **2A–3A** and **2D–3D** and **2A–3C** and **2D–3F**; no transition structure could be found for the C_2–C_6 trapping from either intermediate (**2A** or **2D**) due to the high energy of the primary carbenium ion this process would generate and the availability of low-energy mechanisms with similar geometric features.

In the iso-Nazarov manifold, the two higher energy paths are very close in energy, with activation barriers of 31.32 and 31.69 kcal mol^{-1} (**2D–3D** and **2D–3F**, Table 3). The first one corresponds to the C_1 capture of the carbocation at C_4, followed by a C_7–C_2 semipinacol rearrangement, that results in the more stable protonated bicyclo[3.1.1]hept-2-en-6-one (**3D**). The alternate C_1 capture of the allyl cation at the distal position (C_6) gives rise to a similar process where the initial C_1–C_6 bond formation is followed by a C_4–C_2 semipinacol rearrangement that yields protonated bicyclo[2.2.1]hept-2-en-5-one (**3E**). The similar charge stabilization in the two transition structures helps explain the similarity in the reaction barriers.

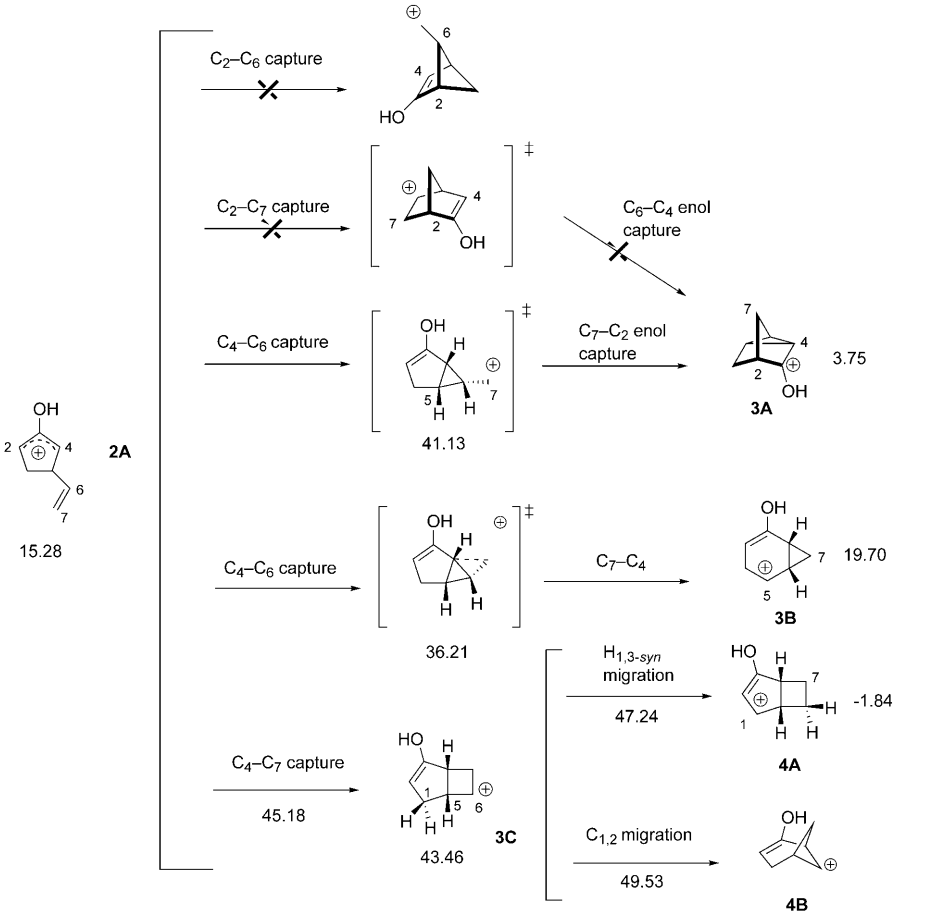

Scheme 6. Intramolecular trapping and further evolution in cationic cascade reactions following the initial Nazarov process of the 3-hydroxyheptatrienyl cation.

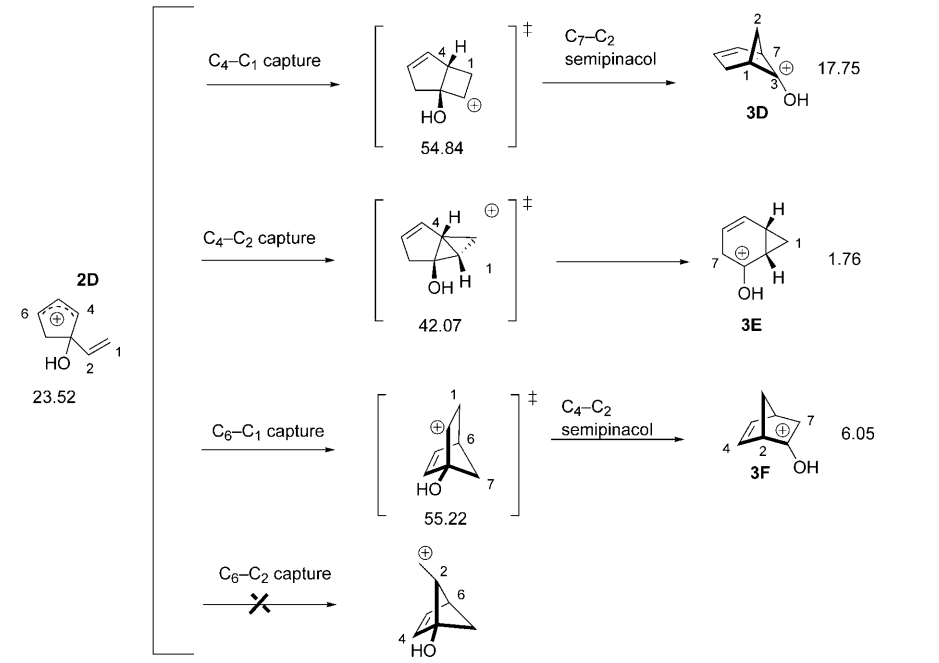

Scheme 7. Intramolecular trapping and further evolution in cationic cascade reactions following the initial iso-Nazarov process of the 3-hydroxyheptatrienyl cation.

Table 3. Thermodynamic data for the mechanistic paths of cationic cascades following the original electrocyclic ring closure of the 3-hydroxyheptatrienyl cation **1**.

Structure	E_e	E_{zpve}	ΔG	$\Delta G^{\neq}$
2A–3A	38.91	39.15	41.13	25.85
2A–3B	33.42	34.51	36.21	20.93
2A–3C	43.38	43.36	45.18	29.90
3C–4A	45.79	45.18	47.24	3.79
3C–4B	47.20	47.61	49.53	6.07
3A	−1.66	1.64	3.75	
3B	17.86	18.39	19.70	
3C	42.18	42.00	43.46	
4B	−5.69	−3.28	−1.84	
2D–3D	54.89	53.38	54.84	31.32
2D–3F	53.76	53.27	55.22	31.69
2D–3E	40.18	40.33	42.07	18.54
3D	13.83	16.12	17.75	
3F	1.23	3.98	6.05	
3E	−1.74	0.25	1.76	

The situation is somehow different for the Nazarov manifold, where the "C_2–C_7" capture[1] is clearly favored with respect to the alternate C_4–C_7 bond-forming process ($\Delta G^{\neq}$ value of 25.85 vs. 29.90 kcal mol^{-1}). The former (**2A–3A**) comprises two concerted events: the formation of a C_6–C_4 bond, and the C_7–C_2 enol capture. Only one bond is formed before a minimum is found in the other two alternatives. The lower barrier for the formation of the distal bridge, which evolves through a concerted transition state to the tricyclic structure **3A** could be attributed to both lower strain in the transition structure and the stabilization that arises of a charge rearrangement that leaves the cation mostly localized as a protonated ketone on the product. The almost simultaneous bond formation could explain the differences between this path and that observed for **2D–3F**, where the normal vibrational mode associated with the imaginary frequency in the transition structure clearly corresponds to the formation of a C_1–C_6 bond.

The third option for the evolution of cyclopentenyl cation **2A** affords bicyclo[3.2.0] **3C** through a transition state corresponding with a single-bond formation step (C_4–C_7 capture). However, this structure can isomerize to the more stable bicyclo[3.2.0] **4A** with a very small activation barrier (3.79 kcal mol^{-1}). From the two processes available and thermodynamically feasible: migration of C_1 to C_6 (the observed evolution of this system in the iso-Nazarov manifold, process **2D–3D**, see Scheme 7) and C_1–H migration, it is the last one which has a lower barrier (3.79 vs. 6.07 kcal mol^{-1}). This unusual 1,3-hydrogen migration is favored before other more conventional processes, such as 1,2-hydrogen or alkyl migration, due to the special geometric disposition of the neighboring atoms in the intermediate, which already has a C_1-C_5-C_6 angle close to that needed in the transition structure (94 vs. 82°) and leaves the *syn* hydrogen on C_1 at a very favorable orientation (74° C_1-H-C_6 angle) and distance from the migration terminus C_6 (2.31 vs. 1.61 Å in the transition structure).

A somewhat similar cascade reaction is reported in the description by West et al. of the "unexpected participation of an unconjugated olefin during Nazarov cyclization of bridged bicyclic dienones",[14] where the product of the reaction can be rationalized as the result of a Nazarov electrocyclization followed by intramolecular trapping of the oxyallyl cation intermediate by a non-conjugated vinyl group and a 1,5-hydride migration.

The favored **2D–3E** reaction path in the iso-Nazarov manifold (see Scheme 7 and Figure 5) is characterized by the tandem formation of the C_2–C_4 and C_1–C_4 and the cleavage of the C_3–C_4 bonds. Although it is a one-step process, the changes in bonding take place rather asynchronously, with the initial formation of a C_2–C_4 bond with some positive charge buildup on C_1 and C_2, followed by migration of the C_3–C_4 bond to C_1, that would formally correspond to a cyclopropylmethyl to cyclopropylmethylene rearrangement also facilitated by the charge stabilization as an oxocarbenium ion. The dramatic increase in the positive charge on C_3, together with the loss of cationic character of C_1 after the transition structure agree with this description.

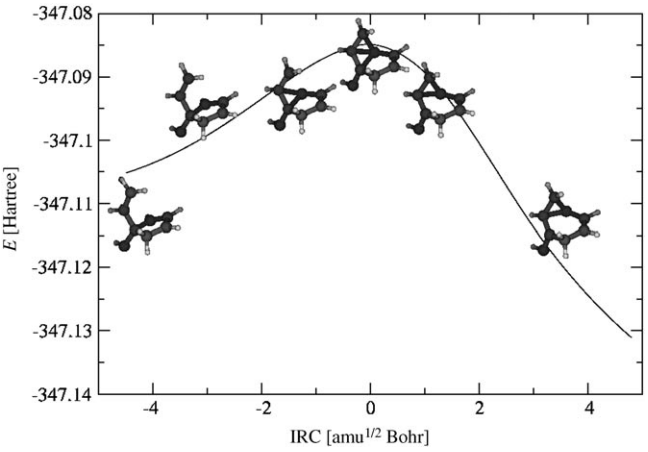

Figure 5. Representation of the evolution of **2D** upon the intramolecular trapping of the cation. Several snapshots of the structure are shown overlying the energy versus reaction coordinate plot.

The variation of the represented C–C distances correlates well with the evolution of the charges along the reaction path (IRC). The formation of C_1–C_4 and breaking of C_3–C_4 correspond to an increased electron density on C_6 (due to localization of the π electrons) and the stabilization of the cation on C_3 by the heteroatom (Figure 6).

The **2A–3B** reaction path is very similar. The main differences in energy and extent of evolution arise from the location of the hydroxyl substituent with respect to the forming and breaking bonds, which strongly affects the charge distribution along the IRC and the energy of both the transition

[1] This is an example of a reaction path that does not conform to the original mechanistic definition. We continue referring to this path as "C_2–C_7" capture, even if what is really happening is the sequential (without intermediates) closing of a C_4–C_6 bond, and formation of the expected C_2–C_7 bond.

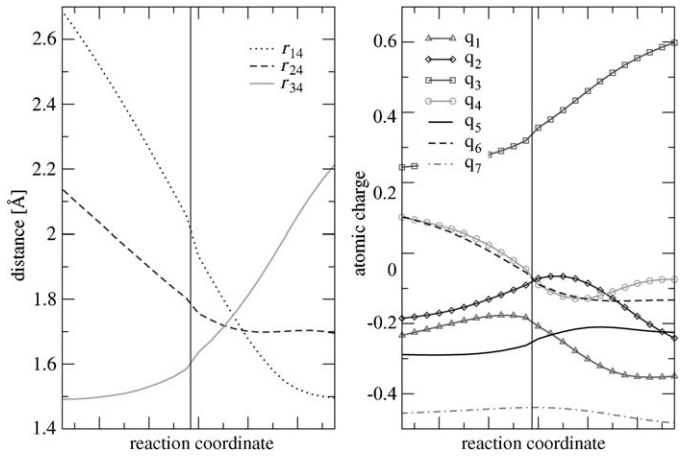

Figure 6. Bond length and NBO atomic charge evolution versus reaction coordinate along the IRC corresponding to **2D**–**3E**.

structure and the minima it connects. Protonated ketone in **3E** is much more stable than the secondary carbenium ion in **3B**, but the starting cyclopentenyl cation **2A** stabilizes better its charge than its counterpart **2D**, which results in both a lower energy starting point and a lower energy transition structure for the evolution of the Nazarov hydroxycyclopentyl cation **2A** (expected from a structure closer to the cyclopentenyl than to the bicyclic product). The shape of the q_4 curve with decreasing positive charge that reaches a minimum near the transition state to increase again afterwards reflects well the forming and breaking of bonds in both processes (Figure 7). Although the variations in q_3 and q_5 in **2D**–**3E** and q_5 and q_3 in **2A**–**3B** (for the comparison we use the geometric equivalent positions, instead of the actual atom numbers on the original structures) display the same overall trend (increasing positive charge buildup), the charge range for q_3 (iso-Nazarov) is much smaller than that corresponding to q_5 (Nazarov). The opposite is true when

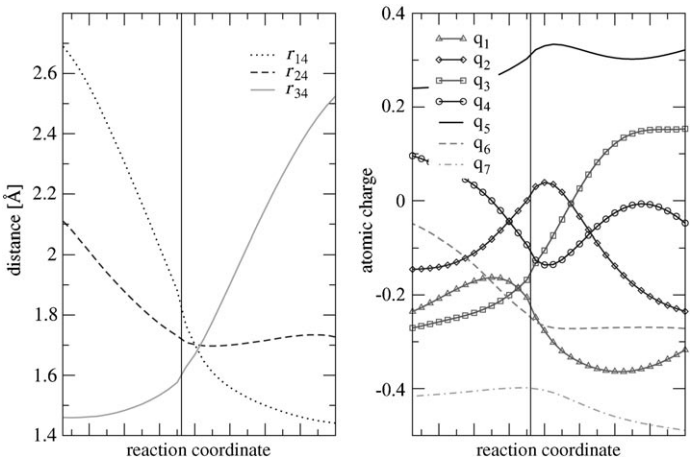

Figure 7. Bond length and NBO atomic charge evolution versus reaction coordinate along the IRC corresponding to **2A**–**3B**.

comparing q_5 (iso-Nazarov) with q_3 (Nazarov), due to the ability of the hydroxyl groups to stabilize positive charge. The main discrepancy between the two plots, the pronounced maximum in q_2 in **2A**–**3B** that finds no counterpart in q6 in **2D**–**3E**, can be ascribed to a resonant form of the enol in the vicinity of **2A**–**3B**, which locates negative charge on C_2.

Cycloisomerization of the 1-hydroxyheptatrienyl cation: As for the previous molecule, we split the study of 1-hydroxyheptatrienyl cation cyclizations in two sets of starting isomers: that where the hydroxy group is located at one of the termini of the cyclizing system (**5E** to **5L**) (it could be considered a 1-hydroxy-5-vinylpentadienyl cation) and that corresponding to a pentadienyl cation with a putative enol substituent, which could be named as a hydroxyvinylpentadienylcation (**5A** to **5D** and **5M** to **5P**).

***Iso-Nazarov reaction**:* A picture similar to that corresponding to the previous system can be drawn for this set of pentannelations. The main difference between them is the controlled relative configuration of the two sp^3 centers formed upon the conrotation. Depending on the initial isomer of **5**, the cyclization yields stereoselectively the *cis* or *trans* pentenyl cation. In the system studied, this chiral information is lost in the second step of the reaction, upon proton migration (see Scheme 8). However, if the 1-hydroxyheptatrienyl chain is substituted on C_2, the stereoselective *syn* 1,2-H migration will translate this chiral information into the relative configuration of the C_5 and C_2 centers.

As described for the $4\pi e^-$ reactions of the 3-hydroxyheptatrienyl cation, the most remarkable effect is the high energy of the transition structures involving inwards rotation of donor groups upon cyclization (Table 4). This preference can be quantified comparing **5F**–**6C** with **5G**–**6D** for data on the effect of a vinyl group, a mild donor (4.82 kcal mol^{-1}) and **5E**–**6C** and **5G**–**6D** for the effect of the hydroxyl substituent. The value of $\Delta\Delta G^{\ddagger}_{\text{in-out}}$ obtained for these last processes, 11.74 kcal mol^{-1}, agrees well with the 11.36 kcal mol^{-1} calculated for the electrocyclization of 1,3-dihydroxy-5-methyl-pentadienyl cation.[15] Since the vinyl and hydroxyl substituents are now in opposing extrema of the reacting chain (for the 3-hydroxyheptatrienyl cation, the vinyl and the hydroxyl groups are on the same atom so there is always a donor group rotating inwards at the cyclization), the contributions of these two effects can be modulated and a wider range of activation energies is found.

Examination of the geometry of these structures yields a description of the charge distribution similar to that of the isomers of 3-hydroxyheptatrienyl cation: the π bonds are "localized" over C_1–C_2, C_4–C_5 and C_6–C_7 and the positive charge is concentrated on C_1 stabilized by the hydroxyl group. In the transition structures, however, the electronic redistribution appears to be more advanced than in the previous systems (the Nazarov mode of the 3-hydroxyheptatrienyl cation electrocyclic manifold), with an important positive charge buildup on C_4 and bond-length patterns that

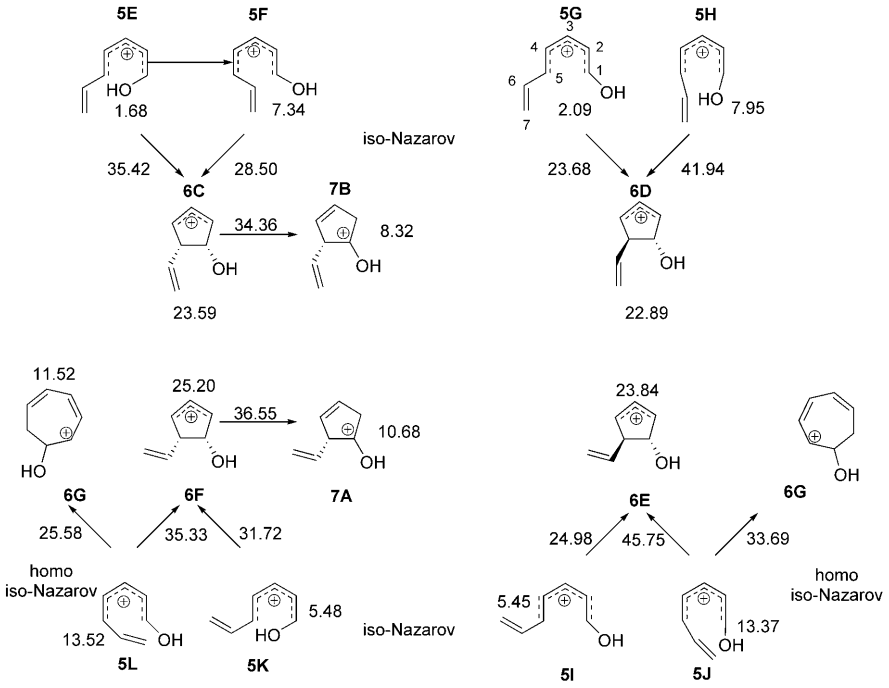

Scheme 8. Iso-Nazarov cyclizations of the 1-hydroxyheptatrienyl cation. The free energies of the depicted stationary points are shown on the scheme in kcal mol^{-1}.

Table 4. Thermodynamic data for the reactions in Scheme 8. The units are kcal mol^{-1} and the reference for relative energies is **5A** (Scheme 9).

Structure	ΔG	$\Delta G^{\neq}$	Structure	ΔG	$\Delta G^{\neq}$
5J	13.37		**6E**	23.84	
5I	5.45		**6F**	25.20	
5K	5.48		**6C**	23.59	
L	13.52		**6D**	22.89	
5E	1.68		**6F–7A**	36.55	11.35
5F	7.34		**6C–7B**	34.36	10.77
5H	7.95		**7A**	10.68	
5G	2.09		**7B**	8.32	
5J–6E	45.75	32.38	**5L–6G′**	37.07	23.55
5I–6E	24.98	19.53	**5L–6G**	25.58	12.07
5K–6F	35.33	29.86	**5J–6G**	33.69	20.32
5L–6F	31.72	18.20	**6G**	11.52	
5E–6C	35.42	33.74	**5F-5L**	17.25	9.91
5F–6C	28.50	21.16	**5J–5L**	33.68	20.31
5H–6D	41.94	33.98			
5G–6D	23.68	21.60			

suggest instead the pattern of an allyl cation and a non conjugated vinyl group.

When comparing the forming bond lengths with those corresponding to their 3-hydroxyheptatrienyl counterparts, we find a higher variability than that of the two sets above discussed, variability that can be accounted for resorting to stereoelectronic effects and the associated consequences in the reaction barriers.

The favored cyclizations for this system, **5G–6D** or **5I–6E** are those leading to the *trans*-hydroxycyclopentenyl product. The energy differences between the three lowest energy transition structures for pentannelation **5G–6D** and **5I–6E** and the transition structure for heptannelation **5L–6G** being low, a mixture of products is expected. From a Maxwell–Boltzmann distribution at 25°, a ratio of 87:10:3 can be predicted for these carbenium ions. Since both pentannelation mechanisms yield the same product, the product ratio would be 97:3, thus ensuring a very high periselectivity for the conrotatory 4e$^-$–5 atom electrocyclic reaction. As explained for the 3-hydroxy analogues, a careful choice of substituents can be expected to modulate the periselectivity of the electrocyclization. The $\Delta\Delta G^{\neq}_{6-4}$ difference, slightly more important than for the isomeric 3-hydroxyheptatrienyl cation cyclizations (1.9 vs. 1.65 kcal mol^{-1}) can be viewed as a compromise between two opposite effects. First, the 4e$^-$ transition structures in the 1-hydroxy system are destabilized, since the more favorable four electron cyclizations of hydroxypentadienyl cations (when the hydroxyl group is located in position C_1 instead of C_3[15]) imply in the transition structures of the 3-hydroxyheptatrienyl system a donor vinyl group rotating inwards. Second, there is loss of cation stabilization when the hydroxyl group is located on a carbon with increasing sp^3 character on the 6e$^-$ transition structure for the 3-hydroxyheptatrienyl cation.

The most interesting feature about these cyclizations is the evolution of the hydroxycyclopentenyl products. The location of the hydroxy group in an sp^3 carbon, with a geminal hydrogen atom, makes available a path that the geminal vinyl group prevented the system from following in the products of the pentannelation of the isomeric 3-hydroxyheptatrienyl cation. With activation barriers of 11.35 and 10.77 kcal mol^{-1} for the *syn* and *anti* products, respectively, a hydrogen atom geminal to the hydroxyl can migrate to the proximal allylic carbon to yield stable protonated 2-vinylcyclopent-3-en-1-ones. When compared to the barriers for the processes available to the hydroxyvinylcyclopentenyl cations **2A** and **2D**, these proton shifts are much more favorable, eliminating rearrangements by other group migrations from the competition.

Cyclization of pentadienyl cations: The favored processes for the electrocyclization of 1-hydroxyheptatrienyl cation however, are those corresponding to the C_3–C_7 ring closure, with barriers of 18.79 and 20.25 kcal mol^{-1} for **5C–6B** and **5A–6A**, respectively. From the comparison between activation barriers calculated[25] for the pentadienyl cation cycliza-

tion and the Nazarov reaction (the cyclization of protonated divinyl ketone), 7.94 and 15.94 kcal mol^{-1} respectively and for the pentannelation of 1-hydroxypentadienyl cation 14.18 kcal mol^{-1} (calculated at the same level, MP2/6-31G*//HF/6-31G*), the lower barrier for the C_3–C_7 cyclization is expected, since the stabilizing effect of the hydroxyl group on the cyclizing system in the reactant is removed and the enol can, in the transition structure, both stabilize the delocalized positive charge and polarize the π system resulting in a certain ionic contribution to the mechanism that lowers the energy of the electrocyclization.[2] However, the most remarkable feature of the electrocyclic reactivity of this system is the uncommon products **6A** and **6B**.

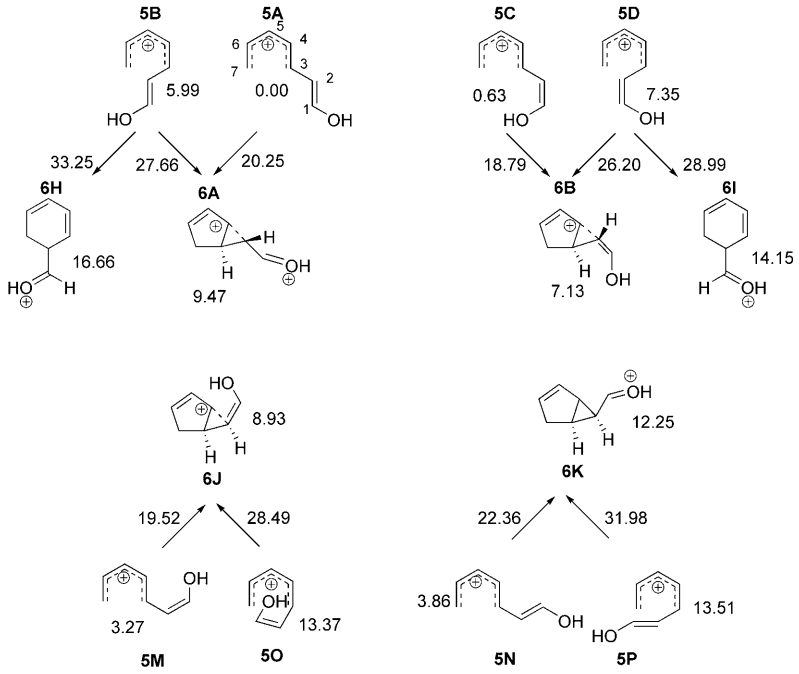

Scheme 9. Pentadienyl cation cyclizations of the 1-hydroxyheptatrienyl cation. The free energies of the depicted stationary points are shown on the scheme in kcal mol^{-1}.

The structure of **6A** is that of a cyclopentenyl cation whose charge deficiency is attenuated by assistance of the π electron density of its enol substituent, resulting in a non-classical carbocation (see Figure 8). Not only the distorted, cyclopropane-like structure suggests a non-classical carbenium ion, but the putative allyl cation is heavily localized due to the anchimeric assistance of the enol, as indicated by its bond lengths (1.35 and 1.46 Å for the non assisted C_5–C_6 and assisted C_4–C_5 bonds, respectively). APT partial charges also reinforce this interpretation, the charge deficiency being largely supported by C_1 and C_4 with partial charges of 0.64 and 1.12 a.c.u., respectively. Despite the strong evidences pointing towards the existence of a chemical bond between C_2 and C_4, further analysis led to contradictory results. Analysis of the topology of the electron density showed no bond critical point between nuclei C_3 and C_4, but the Wiberg bond index matrix obtained in the course of natural bond orbital analysis showed a moderate bond order (0.59). Thus, we came to the conclusion that whereas a considerably strong electrostatic interaction and a certain amount of charge transfer between the allyl cation and the enol moieties exists, the existence of a chemical bond, strictly speaking, could not be ascertained. Similar structures are found for **6B**, **6J** and **6K**, with longer C_2–C_4 distances for **6B** (1.84 Å) and **6J** (2.10 Å), the structures with a *Z* enol (compared to the 1.75 Å of **6A** and **6K**). These longer C_2–C_4 distances could be attributed to a electrostatic interaction between the hydroxyl oxygen and a hydrogen on C_7 (for **6J**) or on C_6 (for **6B**), marked by O–H distances of 2.4 and 2.6 Å, respectively. The inverse correlation between the C_2–C_4 and O–H distances seems to support this assumption.

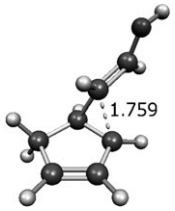

Figure 8. Non-classical carbenium ion **6A**. The non-classical charge transfer interaction (-----) and bond length provided in Ångstroms.

In a recent study on the cyclization of activated (2*E*,4*Z*)-heptatrienoate,[24] we found that the non-classical carbenium ion **6A** is stable and doesn't evolve towards a cyclopropane ring (even if in the presence of a softer Lewis acid such as BF_3, the cyclopropanation step follows the formation of the C_3–C_7 bond in **5A** without an intermediate). In this context, the high energy of this intermediate (9.47 kcal mol^{-1} over the parent **5A**, Table 5) makes the **5A**–**6A** cyclization endothermic and reversible. The same reasoning applies to the **5B**–**6A**, **5B**–**6A**, **5C**–**6B**, **5D**–**6B**, **5M**–**6J**, **5O**–**6J**, **5N**–**6K**, and **5P**–**6K**. As a result, the expected products are those resulting from the iso-Nazarov paths, despite their higher activation energies.

Periselectivity: In addition to the description as a hydroxyvinylpentadienyl cation, the terminal hydroxyl group allows an alternate picture of this system as protonated heptatrienal or protonated 1-formylhexatriene. This flexibility in the conjugated π system results in the availability of three, instead of two possible electrocyclic mechanisms: 4e$^-$–5 atom and 6e$^-$–7 atom, common with the 3-hydroxy system, and a new 6e$^-$–6 atom process. This last reaction, not possible in

[2] This polarization also exists in the C_1–C_5 cyclizations, induced by the hydroxyl group on one of the terminal carbons.

Table 5. Thermodynamic data for the reactions in Scheme 9.

Structure	ΔG	$\Delta G^{\neq}$	Structure	ΔG	$\Delta G^{\neq}$
5A	0.00		**6H**	16.66	
5B	5.99		**6I**	14.15	
5C	0.63		**5A–5B**	19.40	19.40
5D	7.35		**5M**	3.27	
5A–6A	20.25	20.25	**5N**	3.86	
5D–6B	26.20	18.85	**5O**	13.37	
5C–6B	18.79	18.16	**5P**	13.51	
5B–6A	27.66	21.67	**5M–6J**	19.52	16.25
6A	9.47		**5N–6K**	22.36	18.51
6B	7.13		**5O–6J**	28.49	15.12
5B–6H	33.25	27.25	**5P–6K**	31.98	18.47
5D–6I	28.99	21.64	**6J**	8.93	
			6K	12.25	

the 3-hydroxy system due to the lack of stability of a positive charge on C_1, would be described as the disrotatory electrocyclization of hexatriene resulting in protonated 5-formyl-1,3-cyclohexadiene conformers **6H** and **6I**. This reaction, however, needs to overcome a higher barrier than the alternate 4e$^-$ processes, where the carbenium ion can be delocalized over an allyl or dienyl frame, or even the alternate 6 e$^-$ **5L–6G** cyclization.

Conclusions

Model 1- and 3-hydroxy heptatrienyl cations can undergo 4πe$^-$ or 6πe$^-$ electrocyclizations. The preferred path is a pentannelation for the 1-hydroxy isomer, while for the 3-hydroxy structure there can be competition between the two alternatives. Houk's model of torquoselectivity, imparted by the electronic effects of the substituents helps explain the activation energy differences between the alternative 4πe$^-$ electrocyclizations available for each system.

The effect of substituents can either enhance the periselectivity (through steric destabilization of the s-*cis* conformation needed for the cycloheptadienyl cation formation) or reverse it (through the electronic effects of the substituents in the transition structure in the framework of Houk's model).

For the 6πe$^-$ reaction, the favored path is disrotatory, the alternative conrotatory transition structure laying 9.17 kcal mol^{-1} higher in energy. This relatively low $\Delta\Delta G^{\neq}$ is explained with a detailed study of the IRC and the magnetic properties of the "forbidden" transition state. The computations confirm that the antiaromatic character (as proven by NICS calculations) of the forbidden transition state is avoided by selecting instead a complex reaction path (with no intermediates) which involves the incipient formation of a six-membered ring and its evolution (before bond-forming completion) to the expected cycloheptadienyl product.

Two mechanistic alternatives are available for the cyclopentenyl cations obtained from the electrocyclizations: either intramolecular trapping by the non-conjugated vinyl group or 1,3-proton migration, yielding in some cases bicyclic structures of potential synthetic interest. The reaction coordinates of these processes, which in most cases involve complex atomic motions, could correspond to either very asynchronous concerted mechanisms, or two-step reactions with very shallow or non-existent intermediates.

Non-classical carbenium ions and two-step reactions with non-existent intermediates can be found in the 1-hydroxy heptatrienyl cation rearrangement manifold. For this system there is also a new mechanism that competes in the periselectivity contest, but the transition states for the disrotatory 6πe$^-$ cyclization of a protonated formylhexatriene to yield protonated 5-formyl-cyclohexa-1,3-diene are more energetic than those corresponding to the 4πe$^-$ pentannelation processes.

Methods

All computations in this study have been performed using the Gaussian 03 suite of programs.[26] Density functional theory[27–30] (for a description of density functionals as implemented in the Gaussian series of programs, see: ref. [32]) was used with Becke's three-parameter exchange functional[28] and the nonlocal correlation functional of Lee, Yang and Parr[31] (B3LYP) and the 6-311G* basis set. This method was chosen in view of the previous successful application of this approach to describe the transition structures of other pericyclic reactions,[33] and previous DFT calculations for the Nazarov cyclization and its allene variant.[34–37] The stationary points were characterized by means of harmonic analysis, and for all the transition structures, the vibration related to the imaginary frequency corresponds to the nuclear motion along the reaction coordinate under study. In several significant cases intrinsic reaction coordinate (IRC)[38] calculations were performed to unambiguously connect transition structures with reactants and products. Bond orders and atomic charges were calculated with the natural bond orbital (NBO)[39] method.

For the characterization of aromaticity of some transition structures, Schleyer's nucleus independent chemical shift (NICS)[40] values were computed using gauge-independent atomic orbitals (GIAO method).[41]

For the transition structures corresponding to the 6πe$^-$ conrotatory and disrotatory electrocyclizations of the 3-hydroxyheptatrienyl cation, and to the evolution of the Nazarov and iso-Nazarov products of its 4πe$^-$ electrocyclization, points were sampled at constant intervals. The NBO charges and geometric parameters represented in the plots in Figures 3, 6 and 7, origin in single point calculations over these geometries.

In the study of the non-classical carbenium ion **6A**, the bond critical points[42] were calculated from the B3LYP/6-31++G(d,p)//B3LYP/6-311++G(3df,2p) wavefunction and APT charges[43] were obtained at the B3LYP/6-31++G(d,p) level.

Acknowledgement

The authors thank the Centro de Supercomputación de Galicia (CESGA) for generous allocation of computational resources.

[1] H. Pellissier, *Tetrahedron* **2005**, *61*, 6479–6517.
[2] A. J. Frontier, C. Collison, *Tetrahedron* **2005**, *61*, 7577–7606.
[3] M. A. Tius, *Eur. J. Org. Chem.* **2005**, 2193–2206.
[4] C. J. Rieder, R. J. Fradette, F. G. West, *Chem. Commun.* **2008**, 1572–1574.
[5] T. N. Grant, F. G. West, *Org. Lett.* **2007**, *9*, 3789–3792.
[6] A. Rostami, Y. Wang, A. M. Arif, R. McDonald, F. G. West, *Org. Lett.* **2007**, *9*, 703–706.
[7] F. Dhoro, M. A. Tius, *J. Am. Chem. Soc.* **2005**, *127*, 12472–12473.

[8] T. D. White, F. G. West, *Tetrahedron Lett.* **2005**, *46*, 5629–5632.
[9] H. A. Buchholz, A. de Meijere, *Eur. J. Org. Chem.* **1998**, 2301–2304.
[10] S. Giese, L. Kastrup, D. Stiens, F. G. West, *Angew. Chem.* **2000**, *112*, 2046–2049; *Angew. Chem. Int. Ed.* **2000**, *39*, 1970–1973.
[11] Y. Wang, B. D. Schill, A. M. Arif, F. G. West, *Org. Lett.* **2003**, *5*, 2747–2750.
[12] P. Chiu, S. Li, *Org. Lett.* **2004**, *6*, 613–616.
[13] S. E. Denmark, K. L. Habermas, G. A. Hite, *Helv. Chim. Acta* **1988**, *71*, 168–194.
[14] S. Giese, R. D. Mazzola, Jr., C. M. Amann, A. M. Arif, F. G. West, *Angew. Chem.* **2005**, *117*, 6704–6707; *Angew. Chem. Int. Ed.* **2005**, *44*, 6546–6549.
[15] O. Nieto Faza, C. Silva López, R. Álvarez, A. R. de Lera, *Chem. Eur. J.* **2004**, *10*, 4324–4333.
[16] J. A. Bender, A. E. Blize, C. C. Browder, S. Giese, F. G. West, *J. Org. Chem.* **1998**, *63*, 2430–2431.
[17] K. Marx, W. Eberbach, *Chem. Eur. J.* **2000**, *6*, 2063–2068.
[18] B. Lecea, A. Arrieta, F. P. Cossìo, *J. Org. Chem.* **2005**, *70*, 1035–1041.
[19] M. Reisser, G. Maas, *J. Org. Chem.* **2004**, *69*, 4913–4924.
[20] S. Sankararaman, *Pericyclic Reactions—A Textbook. Reactions, Applications and theory*, Wiley-WCH, New York, **2005**, Chapter 6, pp. 393–398.
[21] A. K. Miller, D. H. Byun, C. M. Beaudry, D. Trauner, *Proc. Natl. Acad. Sci. USA* **2004**, *101*, 12019–12023.
[22] A. K. Miller, M. R. Banghart, C. M. Beaudry, J. M. Suh, D. Trauner, *Tetrahedron* **2003**, *59*, 8919–8930.
[23] W. R. Dolbier, H. Koroniak, K. N. Houk, C. Sheu, *Acc. Chem. Res.* **1996**, *29*, 471–477.
[24] C. Silva López, O. Nieto Faza, R. Álvarez, A. R. de Lera, *J. Org. Chem.* **2006**, *71*, 4497–4501.
[25] D. A. Smith, C. W. Ulmer II, *J. Org. Chem.* **1997**, *62*, 5110–5115.
[26] Gaussian 03, Revision B.01, M. J. Frisch, G. W. Trucks, H. B. Schlegel, G. E. Scuseria, M. A. Robb, J. R. Cheeseman, J. A. Montgomery, Jr., T. Vreven, K. N. Kudin, J. C. Burant, J. M. Millam, S. S. Iyengar, J. Tomasi, V. Barone, B. Mennucci, M. Cossi, G. Scalmani, N. Rega, G. A. Petersson, H. Nakatsuji, M. Hada, M. Ehara, K. Toyota, R. Fukuda, J. Hasegawa, M. Ishida, T. Nakajima, Y. Honda, O. Kitao, H. Nakai, M. Klene, X. Li, J. E. Knox, H. P. Hratchian, J. B. Cross, C. Adamo, J. Jaramillo, R. Gomperts, R. E. Stratmann, O. Yazyev, A. J. Austin, R. Cammi, C. Pomelli, J. W. Ochterski, P. Y. Ayala, K. Morokuma, G. A. Voth, P. Salvador, J. J. Dannenberg, V. G. Zakrzewski, S. Dapprich, A. D. Daniels, M. C. Strain, O. Farkas, D. K. Malick, A. D. Rabuck, K. Raghavachari, J. B. Foresman, J. V. Ortiz, Q. Cui, A. G. Baboul, S. Clifford, J. Cioslowski, B. B. Stefanov, G. Liu, A. Liashenko, P. Piskorz, I. Komaromi, R. L. Martin, D. J. Fox, T. Keith, M. A. Al-Laham, C. Y. Peng, A. Nanayakkara, M. Challacombe, P. M. W. Gill, B. Johnson, W. Chen, M. W. Wong, C. Gonzalez, J. A. Pople, Gaussian, Inc., Pittsburgh PA, **2003**.
[27] A. D. Becke, *Phys. Rev. A* **1988**, *38*, 3098–3100.
[28] A. D. Becke, *J. Chem. Phys.* **1993**, *98*, 5648–5652.
[29] R. G. Parr, W. Yang in *Density functional theory of atoms and molecules*, Oxford University Press, Oxford, **1989**.
[30] T. Ziegler, *Chem. Rev.* **1991**, *91*, 651–667.
[31] C. Lee, W. Yang, R. G. Parr, *Phys. Rev. B* **1988**, *37*, 785–789.
[32] B. G. Johnson, P. M. W. Gill, J. A. Pople, *J. Chem. Phys.* **1993**, *98*, 5612–5626.
[33] E. Goldstein, B. Beno, K. N. Houk, *J. Am. Chem. Soc.* **1996**, *118*, 6036–6043.
[34] A. R. de Lera, J. G. Rey, D. Hrovat, B. Iglesias, S. López, *Tetrahedron Lett.* **1997**, *38*, 7425–7428.
[35] B. Iglesias, A. R. de Lera, J. Rodrìguez-Otero, S. López, *Chem. Eur. J.* **2000**, *6*, 4021–4033.
[36] T. Suzuki, T. Ohwada, K. Shudo, *J. Am. Chem. Soc.* **1997**, *119*, 6774–6780.
[37] T. Ohwada, T. Suzuki, S. Koichi, *J. Am. Chem. Soc.* **1998**, *120*, 4629–4637.
[38] C. Gonzalez, H. B. Schlegel, *J. Phys. Chem.* **1990**, *94*, 5523–5527.
[39] E. D. Glendening, A. E. Reed, J. E. Carpenter, F. Weinhold, NBO Version 3.1, **1995**..
[40] P. von R. Schleyer, C. Maerker, A. Dransfeld, H. Jiao, N. J. R. van Eikema Hommes, *J. Am. Chem. Soc.* **1996**, *118*, 6317–6318.
[41] K. Wolinski, J. F. Hinton, P. Peter, *J. Am. Chem. Soc.* **1990**, *112*, 8251–8260.
[42] R. F. Bader in *Atoms in Molecules—A Quantum Theory*, number 22 in The International Series of Monographs on Chemistry, Oxford University Press, Oxford, **1990**.
[43] J. Cioslowski, *J. Am. Chem. Soc.* **1989**, *111*, 8333–8336.

Received: June 10, 2008
Published online: January 2, 2009

